

Learning Spatial Pyramid Attentive Pooling in Image Synthesis and Image-to-Image Translation

Wei Sun and Tianfu Wu

Department of ECE and the Visual Narrative Initiative, North Carolina State University

{wsun12, tianfu_wu}@ncsu.edu

Abstract

Image synthesis and image-to-image translation are two important generative learning tasks. Remarkable progress has been made by learning Generative Adversarial Networks (GANs) [11] and cycle-consistent GANs (CycleGANs) [52] respectively. This paper presents a method of learning Spatial Pyramid Attentive Pooling (SPAP) which is a novel architectural unit and can be easily integrated into both generators and discriminators in GANs and CycleGANs. The proposed SPAP integrates Atrous spatial pyramid [5], a proposed cascade attention mechanism and residual connections [13]. It leverages the advantages of the three components to facilitate effective end-to-end generative learning: (i) the capability of fusing multi-scale information by ASPP; (ii) the capability of capturing relative importance between both spatial locations (especially multi-scale context) or feature channels by attention; (iii) the capability of preserving information and enhancing optimization feasibility by residual connections. Coarse-to-fine and fine-to-coarse SPAP are studied and intriguing attention maps are observed in both tasks. In experiments, the proposed SPAP is tested in GANs on the Celeba-HQ-128 dataset [18], and tested in CycleGANs on the Image-to-Image translation datasets including the Cityscape dataset [9], Facade and Aerial Maps dataset [52], both obtaining better performance.

1. Introduction

Image synthesis is an important task in computer vision which aims at synthesizing realistic and novel images by learning high-dimensional data distributions. Image-to-Image translation is usually built on image synthesis, especially unsupervised translation (i.e., translation with unpaired images). It provides a general framework for many computer vision tasks such as super-resolution [21, 39], image colorization [17], image style generation [52] and image segmentation [38]. Generative adversarial networks

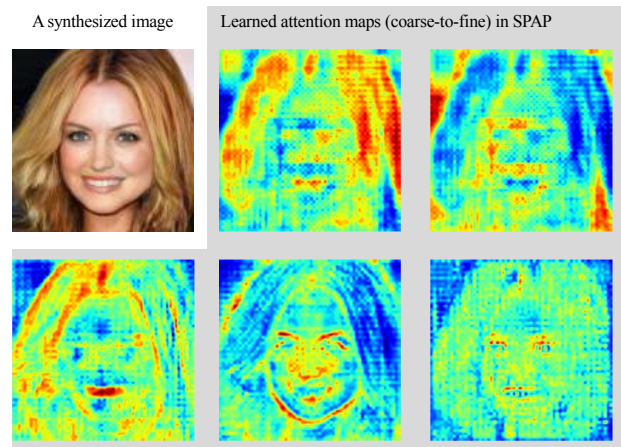


Figure 1: Illustration of the proposed Spatial Pyramid Attentive Pooling (SPAP) in image synthesis using GANs [11] on the Celeba-HQ-128 dataset [18]. The attention maps, visualized using heat maps, are learned in the Atrous spatial pyramid from coarse levels to fine levels (i.e., the dilation rates go from large to small) to fuse different levels. See text for details. (Best viewed in color)

(GANs) [11] are one of the main methods for image synthesis. GANs utilize a two-player game formulation in which one player, the *generator* learns to synthesize images that are indistinguishable from the training data, while the other player, the *discriminator* is trained to differentiate between the generated images and real ones. The generator and discriminator are trained simultaneously by solving a notoriously hard adversarial loss minimax problem. Built on GANs, cycle-consistent GANs (CycleGANs) [52] are one of the main approaches for image-to-image translation. CycleGANs introduce a cycle-consistent loss term into GANs.

Due to the difficulty of solving the minimax problem in practice, many efforts have been devoted to improve the stability of training, the quality of generated images and the capability of generating high-resolution images. Most efforts are mainly focused on loss function design [37, 1, 27, 3,

50, 30], regularization and normalization schema [12, 28], introducing heuristic tricks [36, 31, 14], and training protocol such as the progressively trained GANs [18]. Less attention has been paid to neural architecture design, especially for the generators. The intuitive idea of this paper is that exploring new architectures could improve performance of generative learning in a way complementary to existing efforts. The goal of this paper is to design a generic and light-weight architectural unit that can be easily integrated into both generators and discriminators of GANs and CycleGANs.

The paper presents a spatial pyramid attentive pooling (SPAP) building block which can be used to substitute an existing layer in the generator of a GAN or a CycleGAN. It is built on three ubiquitous components in network architecture design and integrates them in a novel way for generic applicability.

- Atrous convolution or dilated convolutions [4]. The objective is to capture multi-scale information in the input feature map by computing an Atrous spatial pyramid [5]. How to aggregate information in the Atrous spatial pyramid is usually a task-specific problem. For example, in semantic segmentation tasks, they are concatenated together, followed by a 1×1 convolution, so called ASPP to fuse the information in one of the state-of-the-art methods, DeepLab [5]. The ASPP has not been studied in generative learning. However, we observed that this vanilla aggregation is not good enough for generative learning tasks. So, we propose to integrate attention mechanism in the pyramid.
- Self-attention mechanism [48]. It has been recently studied in GANs with significant performance improvement [48]. It modulates response at a position as a weighted sum of features at all positions with learned weights (i.e., a simple position-wise fully connected layer). It is not straightforward to extend this type of self-attention to aggregate multi-scale information. We proposed a novel cascade based scheme to integrate information between successive levels in the pyramid, either coarse-to-fine or fine-to-coarse. Fig. 1 shows an example of synthesized face and the corresponding learned coarse-to-fine attention maps. The proposed cascade attention scheme implicitly implements the progressive training ideas [18]. We show in our experiments that the proposed cascade attention is more effective than the vanilla ASPP method [5].
- Residual connections [13]. We adopt a convex combination between the attention modulated information and the original input information, as done in [48]. The weight is learned. This residual connection will help

both exploit original information and keep the feasibility of optimization.

In summary, the proposed SPAP building block harnesses the advantages of the above stated components in generative learning tasks. In experiments, the proposed method is tested in both image synthesis tasks using the state-of-the-art SNDCGANs [20], and unpaired image-to-image translation tasks using the popular CycleGANs [52]. We obtain significantly better performance than the vanilla SNDCGANs and CycleGANs and the baseline ASPP [5] module. Although our models are much smaller, we obtain comparable performance to the most recent extension of CycleGANs, the SCAN [46] which use stacked CycleGANs in the progressive training protocol.

2. Related Work and Our Contributions

We first briefly overview GANs based generative learning and the related applications of Atrous convolution and attention mechanism.

Generative Adversarial Networks Generative Adversarial Networks (GANs) have achieved great success in various image generation tasks, including image-to-image translation [17, 52, 41, 24, 16], image super-resolution [21, 40] and text-to-image synthesis [34, 35, 46]. Despite the success, the training of GANs is notorious to be unstable and sensitive to the choices of hyper-parameters. Several directions have attempted to stabilize the training of GAN and improve the generated sample diversity, including designing new network architectures [33, 49, 18], modifying the learning objectives and dynamics [37, 1, 27, 3, 50, 30], adding regularization methods [12, 28] and introducing heuristic tricks [36, 31, 14]. Recently spectral normalized model together with projection-based discriminator [29] and [2] greatly improves class-conditional image generation on ImageNet.

Atrous Convolution Atrous convolution is first introduced in [4] to increase receptive field while keeping the feature map resolution unchanged. Atrous Convolution (Dilated Convolution) which can effectively incorporate surrounding context by enlarging receptive field size of kernels, has been explored in image segmentation [5, 6, 7] and object detection [32, 10, 15, 23]. Atrous Spatial Pyramid pooling (ASPP) [7, 6, 5], which exploits the multi-scale information by applying several parallel atrous convolution with different rates, has proved performance on segmentation tasks and promising results on several segmentation benchmarks. DenseASPP [45] connects a set of atrous convolution layers in a dense way, which effectively generates features that covers a large range. In [43], multiple dilated convolutional blocks of different rates are applied for dense object localization and then weakly supervised semantic segmentation. In this paper, we adopt multi atrous convolution

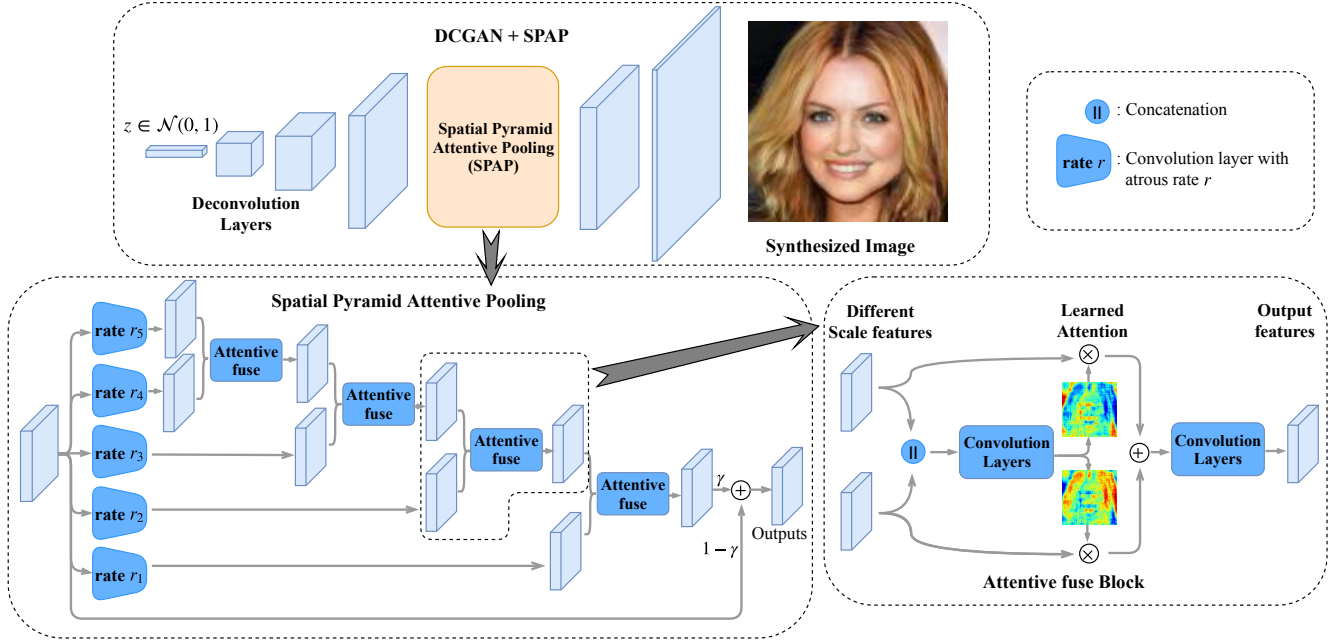


Figure 2: The proposed Spatial Pyramid Attentive Pooling (SPAP) building block. *Top*: Illustration of the integration of the proposed SPAP in the generator of an unconditional GAN for image synthesis. *Bottom-left*: The detailed neural architecture of the proposed SPAP. *Bottom-right*: The operation of the attentive fuse component between two consecutive levels in the pyramid.

to increase the ability of Generator \mathbb{G} and Discriminator \mathbb{D} .

Attention Models Recently attention mechanisms has been exploited in many tasks, including VQA [46] and image classification [51, 44]. SA-GAN [48] first exploit attention to GAN by adding self-attention block to Generator and Discriminator to improve the ability of network to model global structure. In this work, we apply spatial attention when fusing feature maps from different atrous convolution layers in generator \mathbb{G} .

Our Contributions. This paper makes the following two main contributions to the field of generative learning.

- It presents a novel architectural building block, namely spatial pyramid attentive pooling (SPAP), which integrates Atrous spatial pyramid for capturing multi-scale information, a cascade attention scheme for fusing information between multi-scale levels in the pyramid, and a residual connection for feature reuse and enhancing optimization feasibility. To our knowledge, it is the first work that investigates the effects, for generative learning tasks, of Atrous spatial pyramid and the cascade attentive fusion of information from different levels in the pyramid.
- It shows better performance in a series of image synthesis tasks and image-to-image translation tasks.

3. The Proposed Method

In this section, we first briefly introduce the background of GANs and CycleGANs to be self-contained. Then, we present the proposed SPAP module.

3.1. Background

Unconditional GAN A GAN consists of a generator (\mathbb{G}) that map random noise z to samples and a discriminator (\mathbb{D}) that distinguishes the generated samples from the real samples. For unconditional GANs, the basic framework can be viewed as a two-player game between \mathbb{G} and \mathbb{D} , and the objective is to find a Nash equilibrium to the min-max problem,

$$\min_G \max_D \mathbf{E}_{x \sim q(x)} [\log D(x)] + \mathbf{E}_{z \sim p(z)} [\log(1 - D(G(z)))] \quad (1)$$

where $z \in \mathbb{R}^{d_z}$ is a latent variable from distributions such as $\mathcal{N}(0, 1)$ or $\mathcal{U}[-1, 1]$. For generation model on images, deconvolution and convolution neural networks are usually utilized in Generator \mathbb{G} and Discriminator \mathbb{D} respectively.

Image-to-Image translation with CycleGAN GANs have shown improved results in image to image translation tasks [17, 47]. Recent work by Zhu. *et al* [52] has tackled the unpaired image-to-image translation task with a combination of adversarial and cycle-consistency losses. Let's consider two domain X and Y , the CycleGAN model contains two translator model \mathbb{G} and \mathbb{F} which map $X \rightarrow Y$

and $Y \rightarrow X$ respectively. The model has two additional adversarial discriminators \mathbb{D}_X and \mathbb{D}_Y aiming to between real images and translated images in each domain. The loss function of translator and discriminator can be expressed as

$$\begin{aligned} \mathcal{L}_{GAN}(G, D_X, X, Y) = & \mathbf{E}_{y \sim p_{data}(y)}[\log D_Y(y)] \\ & + \mathbf{E}_{x \sim p_{data}(x)}[\log(1 - D_Y(G(x)))] \end{aligned} \quad (2)$$

$$\begin{aligned} \mathcal{L}_{cyc}(G, F) = & \mathbf{E}_{x \sim p_{data}(x)}[\|F(G(x)) - x\|_1] \\ & + \mathbf{E}_{y \sim p_{data}(y)}[\|G(F(y)) - y\|_1] \end{aligned} \quad (3)$$

and full objective of CycleGAN is:

$$\begin{aligned} \min_{G, F} \max_{D_X, D_Y} \mathcal{L}(G, F, D_X, D_Y) = & \mathcal{L}_{GAN}(G, D_Y, X, Y) \\ & + \mathcal{L}_{GAN}(F, D_X, Y, X) \\ & + \lambda \mathcal{L}_{cyc}(G, F) \end{aligned} \quad (4)$$

3.2. The Proposed SPAP

As we briefly discussed in the introduction, our method is motivated by Atrous Spatial Pyramid Pooling (ASPP) [5] where parallel atrous convolution layers with different rates capture multi-scale information. Most of GANs and related models for image generation and translation tasks are based on convolutional layers with small kernels (3×3 or 4×4) in order to keep both computation and the number of parameters contained. Small kernel convolution process information in a neighborhood. Multi-scale information captured by atrous convolution should also improve performance of image synthesis with GANs.

Figure 2 illustrates the structure of our SPAP module and its integration in an unconditional GAN structure. In the intermediate feature of the model, we apply several parallel convolution layers with different atrous rate, of which each capture different scale information. In ASPP module of image segmentation model, the features extracted are further processed and fused by channel concatenation and 1×1 convolution. Image synthesis task is different from segmentation, and we know that different regions in the image should focus on different scale information. Spatial attention is not included in 1×1 convolution. In our module, we design an attentive fuse component to two feature maps of different scale each time. For the attentive fuse layer, as shown in top right of Fig. 2, giving feature maps of two convolution layers f_i and f_{i+1} , we introduce a spatial attention layer to learn a dynamic combination of the two features,

$$AttenFuse(f_i, f_{i+1}) = f_i \odot \alpha_i + f_{i+1} \odot (1 - \alpha_{i+1}) \quad (5)$$

where $\alpha_i = Atten(f_i, f_{i+1})$ indicates the pixel-wise attention map predicted by sequence of convolutional neural network followed by sigmoid activation, and \odot means

element-wise product. Then fused multi-scale feature is added to the input feature map by a learnable scale parameter γ , so the final output would be,

$$y_{out} = \gamma * o + (1 - \gamma) * x_{in} \quad (6)$$

For the order of fusing different scale features, we experiment with various ways. For larger dilate convolution rate, the results are coarse. So we experiment with direction of coarse-to-fine as well as fine-to-coarse.

Discriminator. The proposed SPAP module can be used in discriminator too. However, we observed that it is more important to improve the expressive power of generators in GANs and the job for discriminator is relatively simpler (i.e., binary classification between real vs fake). In addition, it will be clearer to show the capability of the proposed SPAP module if we use it only in generators, as well as for simplicity. That being said, we use much simpler aggregation scheme for discriminator. We only utilize atrous convolution since it can also increase the receptive field and improve the discriminative capability. Vanilla ASPP module used in segmentation network will introduce more parameter and make \mathbb{D} harder to train. Following the idea of [43], we add several parallel dilation convolutions to discriminator in a simple way. As shown in Fig. 3, inside blue rounded rectangle are layers included in the original discriminator, and red ones are added atrous convolution layers. For a specific convolution layer, we can add several parallel convolutions with various atrous rates, then these layers are included in the whole network by calculating mean of outputs, and finally average with the origin no-atrous convolution layer. With this structure, we can effectively increase the receptive field of convolutional network without introducing too many parameters.

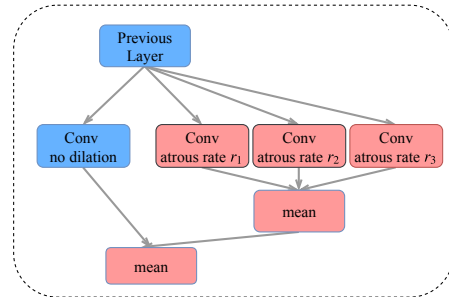


Figure 3: Adding atrous convolution to discriminator

4. Experiments

We test the proposed SPAP module in a series of generative learning tasks.

4.1. Datasets

CELEBA-HQ CelebA-HQ is a high quality version of CelebA dataset, which consists of 30000 of the images in 1024x1024 resolution [18]. We use the 128x128x3 version obtained by the code provided by the author¹, randomly split 27000 images as training dataset and remaining 3000 image as testing dataset.

Image-to-Image Translation To demonstrate the capability of our proposed SPAP module in GAN related networks, we test on unsupervised image-to-image translation problem with CycleGAN model [52]. We conduct experiments on Cityscapes Labels \Leftrightarrow Photo, Maps \Leftrightarrow Aerial, Facades \Leftrightarrow Labels and Horse \Leftrightarrow Zebra datasets. We compare with CycleGAN and SCAN [22] and Pix2Pix [17] results on 256x256 resolution images.

4.2. Evaluation Metrics

Fréchet Inception distance (FID) FID score was introduced in [14]. Samples from \mathcal{X} and \mathcal{Y} are first embedded into a feature space by a specific later of Inception-Net. Both these feature distributions are modeled as multi-dimensional Gaussians parameterized by their respective mean and covariance. Then the Fréchet distance is measured by

$$\text{FID} = \|\mu_x - \mu_y\|^2 + \text{Tr}(\Sigma_x + \Sigma_y - 2(\Sigma_x \Sigma_y)^{\frac{1}{2}})$$

where (μ_x, Σ_x) and (μ_y, Σ_y) denote the mean and covariance of the real and generated image distributions respectively. FID score is used to evaluate generative models for no-labeled data and is robust to various manipulations and sensitive to mode dropping [26].

FCN Segmentation Score For Cityscape Label \Leftrightarrow Photo dataset, we apply segmentation scores to evaluates how interpretable the translated photos. An off-the-shelf FCN segmentation network [25] is applied to the translated images for predicting labels, then three standard segmentation metrics is calculated against the ground truth labels, including per-pixel accuracy, the per-class accuracy and the mean class accuracy.

PSNR and SSIM For Facade \Leftrightarrow Label and Maps \Leftrightarrow Label dataset, we calculate PSNR and SSIM [42] for quantitative evaluation. PSNR can measure color similarity and SSIM can measure structural similarity between translated images and ground truth.

4.3. Network Structure and Implement Details

For unconditional image generation network, we follow the SNDCGAN setting of [20]. Spectral norm is applied [28] to both generator and discriminator. For all models,

¹Code available at https://github.com/tkarras/progressive_growing_of_gans

we use the Adam optimizer [19], learning rate for discriminator and generator are 0.0002 and 0.0001. Batch size is set as 64 and total training steps are 100k. When deploying SPAP, we add one module after the 64x64 size feature map of generator, and also add parallel atrous convolution layer in second downsample layer of discriminator as show in Fig. 3.

For image-to-image translation task, we adopt the network structure setting of [52]. For 256×256 images, the generator network contains two stride-2 convolution, 9 residual blocks and two deconvolution layers with stride $\frac{1}{2}$. We conduct one SPAP module after the first upsample deconvolution layer, which has a feature map size of 128x128. For discriminator, three atrous convolutions are deployed to the third convolution layer, where the input feature map size is 64x64, to increase discriminative ability. Adam optimizer [19] with $\beta_1 = 0.5$ and $\beta_2 = 0.999$ is applied, learning rate set as 0.0002 for the first 100 epoch and linearly decay to zero in the next 100 epoches.

For SPAP module, we apply three 3×3 atrous convolutions with different rates, one 3×3 and then one 1×1 convolution without atrous rate 1. For image generation on CelebA-HQ, we adopt rates (3, 5, 7) and for image-to-image translation task, a larger atrous rate (6, 12, 18) is applied where images resolution is higher. For both tasks, rates are set to (3, 5, 7) when deploying atrous convolution to discriminator \mathbb{D} . For all experiments, we start to update the parameters of SPAP and Atrous convolution after a number of training steps (40k steps for unconditional GAN and 100 epoch for CycleGAN model.)

4.4. Experimental Results

Unconditional GAN on CelebA-HQ Sample of Generated images and its related FID score is show in Fig. 4. Table 1 shows Fréchet Inception Distance (FID) with SNDCGAN + SPAP, compared with SNDCGAN [20] and Self-Module [8]. By just adding vanilla ASPP module to both generator and discriminator, FID score can be improved to 22.55, whiling applying SPAP in a coarse-to-fine order to generator and dilated convolutions to discriminator in SNDCGAN structure significantly improve FID score from 25.42 to 18.47. SPAP module in fine-to-coarse order also improve the FID score to 19.73. This improvement demonstrate the effectiveness of the proposed SPAP in \mathbb{G} and Atrous in \mathbb{D} mechanism.

Table 1: FID score on CELEBA-HQ (smaller is better)

Model	Parameters in \mathbb{G}	Best	Median
Vanilla SNDCGAN	20.065M	25.42	26.11
SELF-MOD [8]	-	22.51	-
SNDCGAN+ASPP	20.762M	20.07	21.26
SNDCGAN+SPAP (fine to coarse)	20.756 M	19.73	20.73
SNDCGAN+SPAP (coarse to fine)	20.756 M	18.47	20.11

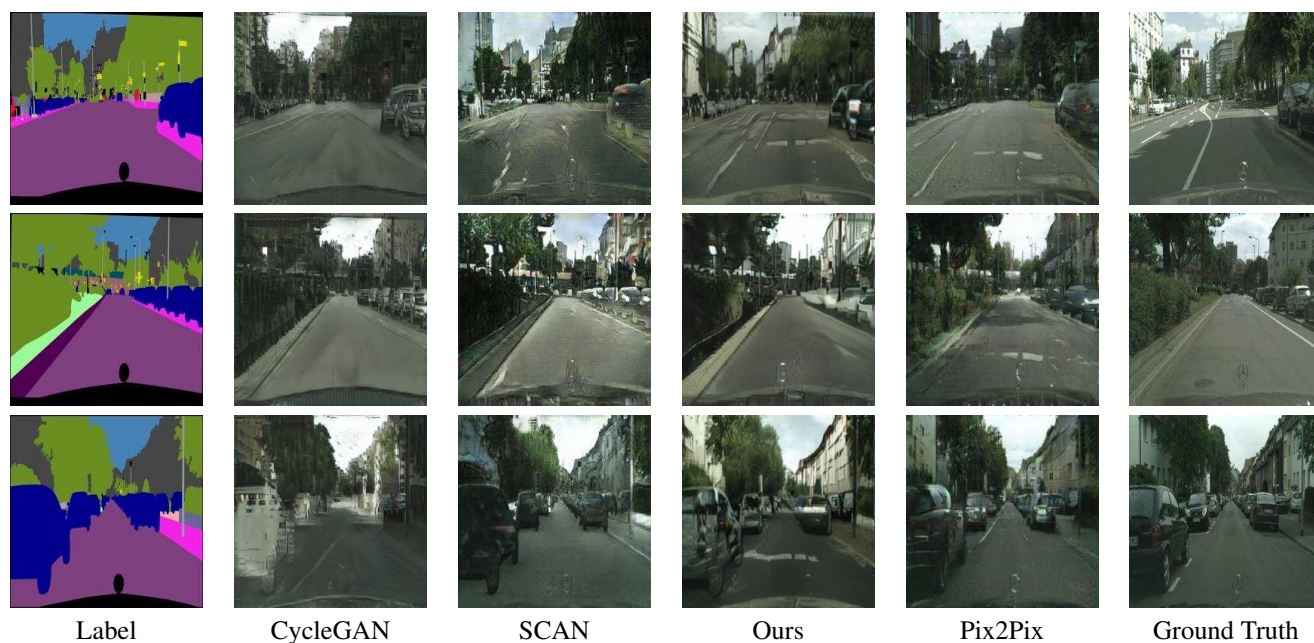


SPAP FID: 18.47

ASPP FID: 22.55

Vanilla FID: 25.42

Figure 4: Examples of generated images by the proposed model trained on CelebA-HQ.



Label

CycleGAN

SCAN

Ours

Pix2Pix

Ground Truth

Figure 5: Comparisons on Cityscapes dataset of 256x256 resolution. Images of CycleGAN and SCAN from [22]. Our results generated with SPAP in coarse-to-fine order.

Table 2: FCN segmentation scores on Cityscape Photo \leftrightarrow Label

Method	Labels \Rightarrow Photo			Photo \Rightarrow Label		
	Pixel acc.	Class acc.	Class IoU	Pixel acc.	Class acc.	Class IoU
CycleGAN	0.52	0.17	0.11	0.58	0.22	0.16
ASPP	0.52	0.17	0.12	0.53	0.18	0.13
SPAP(fine-to-coarse)	0.71	0.20	0.15	0.66	0.20	0.16
SPAP(coarse-to-fine)	0.73	0.22	0.17	0.71	0.25	0.19
SCAN	0.64	0.20	0.16	0.72	0.25	0.20
Pix2Pix	0.71	0.25	0.18	0.85	0.40	0.32

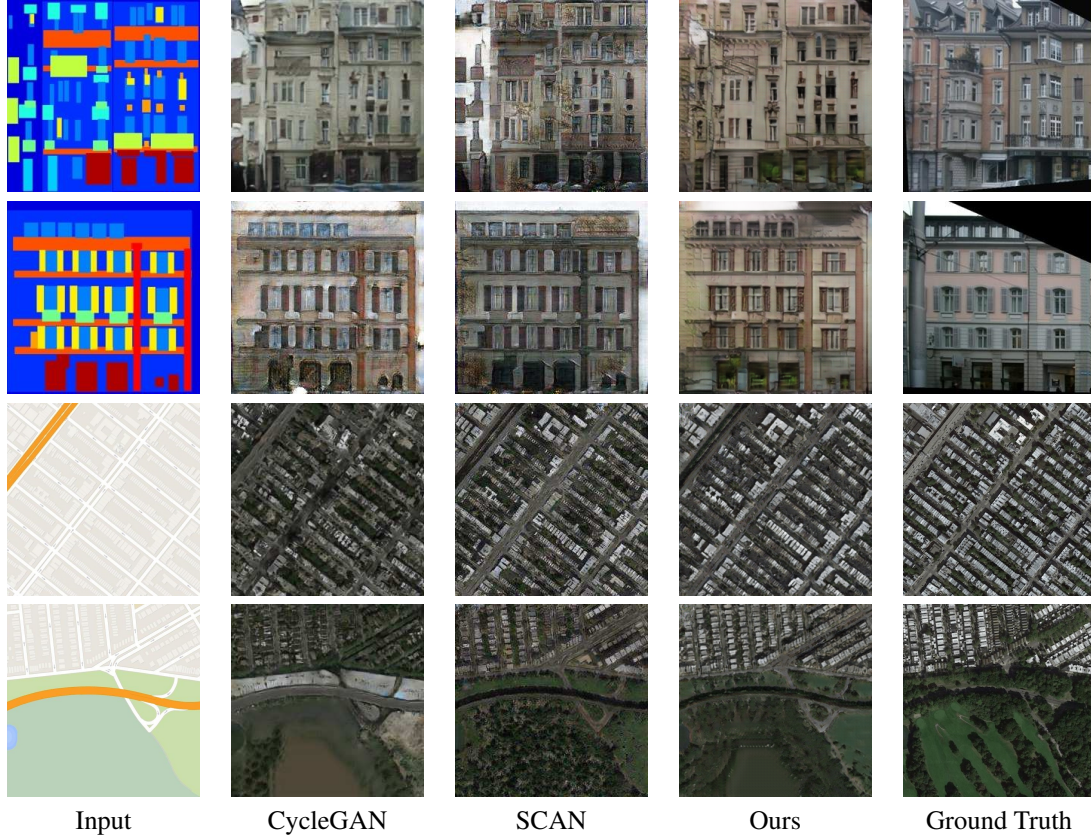


Figure 6: Results on Labels \Rightarrow Facades and Labels \Rightarrow Maps. CycleGAN and SCAN images from paper [22]. Our results generated with SPAP in coarse-to-fine order.

Table 3: PSNR and SSIM values Map \Leftrightarrow Aerial and Facades \Leftrightarrow Labels. Note that SCAN has much bigger models since it uses stacked CycleGANs without sharing parameters

Method	Aerial \Rightarrow Map		Map \Rightarrow Aerial		Facades \Rightarrow Labels		Labels \Rightarrow Facades	
	PSNR	SSIM	PSNR	SSIM	PSNR	SSIM	PSNR	SSIM
CycleGAN	24.68	0.63	14.39	0.20	8.73	0.33	11.72	0.20
ASPP	24.33	0.65	14.62	0.21	7.69	0.26	11.65	0.14
SPAP(fine-to-coarse)	24.95	0.66	14.47	0.21	9.00	0.35	11.65	0.19
SPAP(coarse-to-fine)	25.02	0.66	14.40	0.22	9.21	0.35	12.20	0.21
SCAN	25.15	0.67	14.93	0.23	8.28	0.29	10.67	0.17

Image-to-Image translation with CycleGAN Fig. 5 visually compare our results with CycleGAN, SCAN and Pix2Pix. Images generated by SPAP in coarse-to-fine order are more realistic and vivid, and closer to Pix2Pix and ground truth when compared with CycleGAN. This quality improvement are further illustrated in Table. 2, where our model outperforms SCAN and CycleGAN on Label \Rightarrow Image generation, even close to Pix2Pix which is trained on paired data. Our model also outperform CycleGAN on Photo \Rightarrow Label and gets comparable results with SCAN.

Fig. 6 shows selected generated sample results in the Aerial \Rightarrow Map and the Labels \Rightarrow Facades task. We can ob-

serve that our results contains better image quality and finer pattern. Table. 3 shows quatitive evaluation metric PSNR and SSIM on Map \Leftrightarrow Aerial and Facades \Leftrightarrow Labels dataset, which proves that our image synthesis results are more similar to ground truth in terms of colors and structures than CycleGAN, and results are comparable to SCAN.

4.5. Analysis of Attention module in Generator \mathbb{G}

Fig. 7 and 8 illustrates selected synthesized samples from GAN with SPAP module and visualization of attention map when fusing different feature maps in coarse-to-fine order, and Fig. 9 shows attention maps in fine-to-coarse order

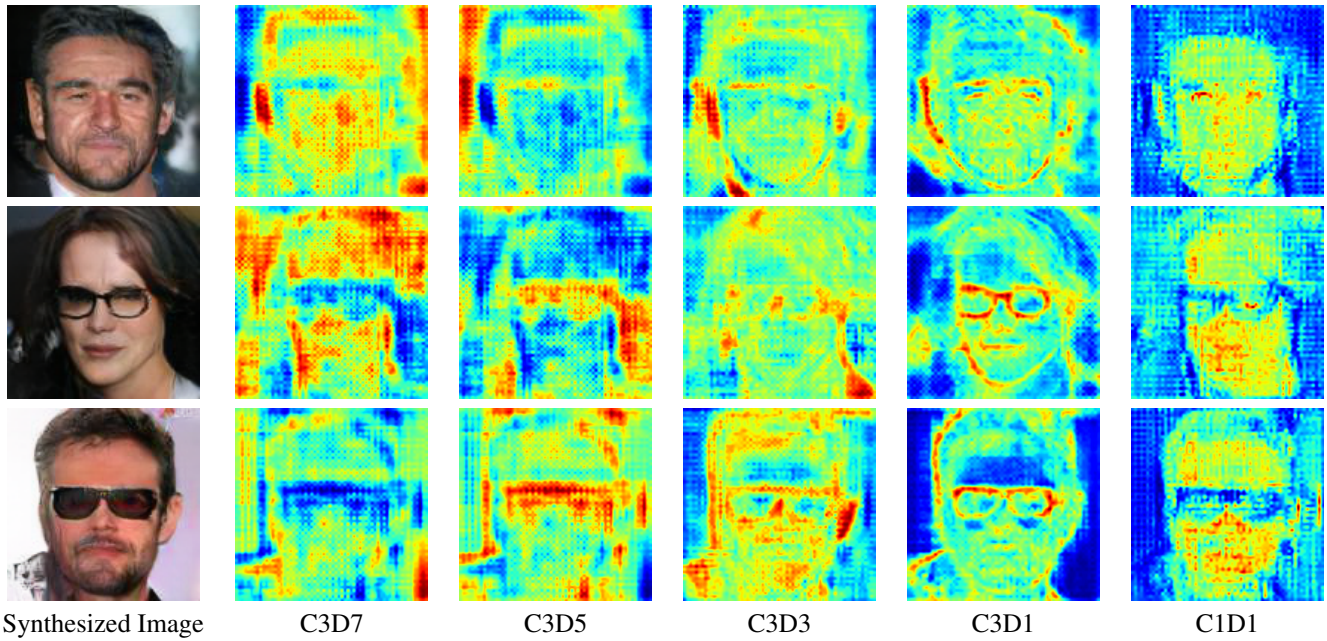


Figure 7: Selected samples of synthesized images and visualization of attention map for SPAP in coarse-to-fine order. $CkDn$ denotes $k \times k$ Convolution layer with atrous rate n .

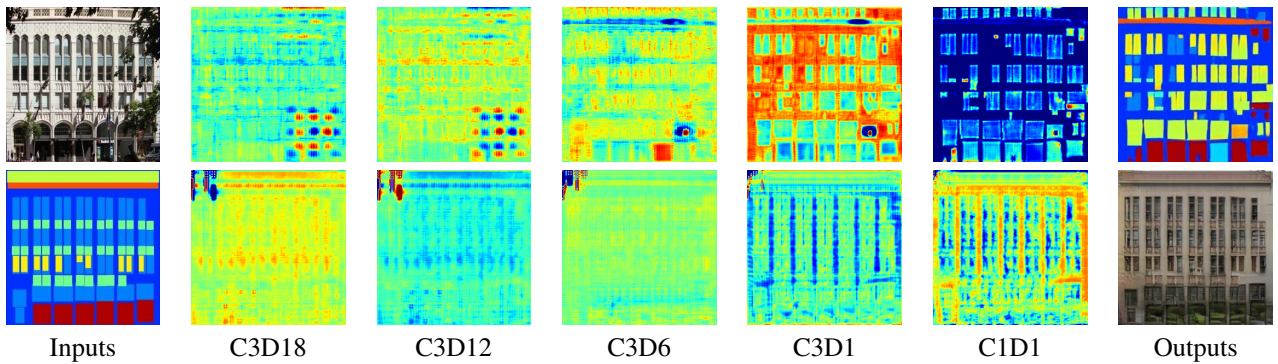


Figure 8: Selected samples of synthesized images and visualization of attention mapS for SPAP in coarse-to-fine order.

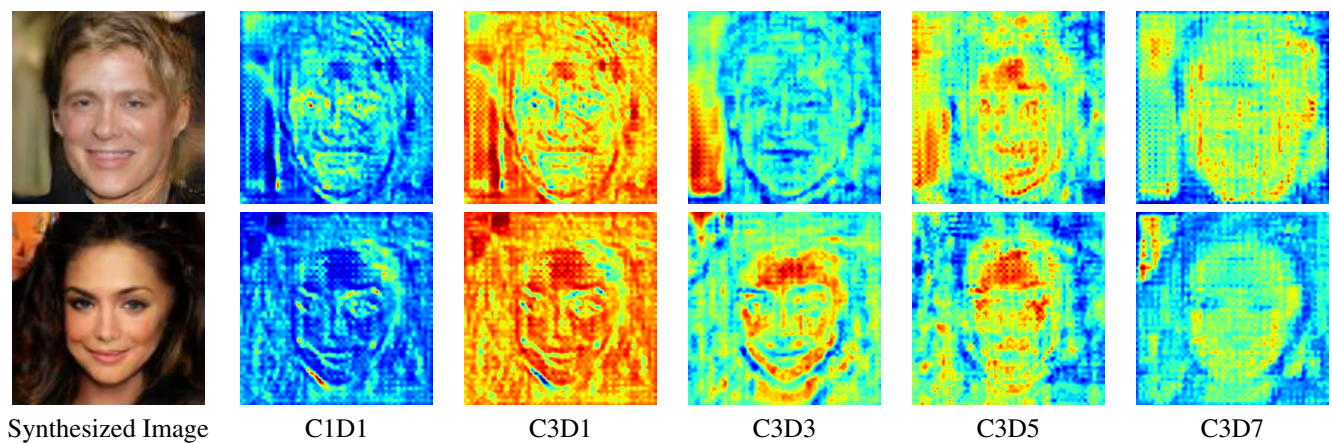


Figure 9: Selected samples of synthesized images and visualization of attention map for SPAP in fine-to-coarse order.

SPAP. These figures can clearly demonstrate effectiveness of spatial attention in SPAP to fuse different scale information. In face generation in Fig. 7, where SPAP is fused in a coarse-to-fine order, for features of large atrous rates, the model tends to focus more on region like background, hair, etc., while for features of small atrous rates, attention value is high on contour of face, glasses, eyes, etc.

4.6. Analysis of Receptive field in Discriminator \mathbb{D}

For CycleGAN and Pix2Pix [17], PatchGAN is used as discriminator, with a 70x70 receptive field. The PatchGAN only penalizes structure at the scale of patches, it tries to classify if each NxN patch in an image is real or fake. Such a discriminator effectively models the image as a Markov random field, assuming independence between pixels separated by more than a patch diameter. In this paper, we add three parallel convolution with different atrous rates, which will increase the receptive field of the PatchGAN. If we add stride-2 convolution with atrous rate 3,5,7 at 64x64 feature map, the receptive field of discriminator will increase to 236x236. In [17], full 286x286 ImageGAN produce a lower FCN-score which, to their opinion, might because that ImageGAN having more parameters and greater depth make it harder to train. In our model, the added atrous convolution can effectively increase the receptive field without adding too many parameters or increasing depth of the model.

In vanilla SNDCGAN, the receptive field of the convolution before the final fully connected layer is 52. If we add SPAP layer to the model, the receptive field will be increased to 100 by stride-2 convolution with atrous rate 7 in 64x64 feature map.

5. Conclusions

This paper proposed an spatial pyramid attentive pooling (SPAP) building block which can be integrated into both generators and discriminators in GANs based generative learning. The proposed SPAP is a simple yet effective module which harnesses the advantages of three ubiquitous components in neural architecture design in a novel way: Atrous spatial pyramid for capturing multi-scale information, a cascade attention scheme for aggregating information between different levels in the pyramid, and residual connections. The proposed SPAP module is complementary to many existing efforts towards building more accurate and more robust GANs based generative learning models. In experiments, we test our method on unconditional GANs with the Celeba-HQ-128 dataset and unpaired image-to-image CycleGANs with the CityScape, Facade, Maps dataset, all obtaining better or comparable performance than state-of-the-art models.

Acknowledgment. This work is supported by ARO award W911NF1810295, ARO DURIP award W911NF1810209 and NSF IIS 1822477.

References

- [1] Martin Arjovsky, Soumith Chintala, and Léon Bottou. Wasserstein gan. *arXiv preprint arXiv:1701.07875*, 2017. 1, 2
- [2] Andrew Brock, Jeff Donahue, and Karen Simonyan. Large scale gan training for high fidelity natural image synthesis. *arXiv preprint arXiv:1809.11096*, 2018. 2
- [3] Tong Che, Yanran Li, Athul Paul Jacob, Yoshua Bengio, and Wenjie Li. Mode regularized generative adversarial networks. *arXiv preprint arXiv:1612.02136*, 2016. 1, 2
- [4] Liang-Chieh Chen, George Papandreou, Iasonas Kokkinos, Kevin Murphy, and Alan L Yuille. Semantic image segmentation with deep convolutional nets and fully connected crfs. *arXiv preprint arXiv:1412.7062*, 2014. 2
- [5] Liang-Chieh Chen, George Papandreou, Iasonas Kokkinos, Kevin Murphy, and Alan L Yuille. Deeplab: Semantic image segmentation with deep convolutional nets, atrous convolution, and fully connected crfs. *IEEE transactions on pattern analysis and machine intelligence*, 40(4):834–848, 2018. 1, 2, 4
- [6] Liang-Chieh Chen, George Papandreou, Florian Schroff, and Hartwig Adam. Rethinking atrous convolution for semantic image segmentation. *arXiv preprint arXiv:1706.05587*, 2017. 2
- [7] Liang-Chieh Chen, Yukun Zhu, George Papandreou, Florian Schroff, and Hartwig Adam. Encoder-decoder with atrous separable convolution for semantic image segmentation. *arXiv preprint arXiv:1802.02611*, 2018. 2
- [8] Ting Chen, Mario Lucic, Neil Houlsby, and Sylvain Gelly. On self modulation for generative adversarial networks. *arXiv preprint arXiv:1810.01365*, 2018. 5
- [9] Marius Cordts, Mohamed Omran, Sebastian Ramos, Timo Rehfeld, Markus Enzweiler, Rodrigo Benenson, Uwe Franke, Stefan Roth, and Bernt Schiele. The cityscapes dataset for semantic urban scene understanding. In *Proceedings of the IEEE conference on computer vision and pattern recognition*, pages 3213–3223, 2016. 1
- [10] Jifeng Dai, Yi Li, Kaiming He, and Jian Sun. R-fcn: Object detection via region-based fully convolutional networks. In *Advances in neural information processing systems*, pages 379–387, 2016. 2

- [11] Ian Goodfellow, Jean Pouget-Abadie, Mehdi Mirza, Bing Xu, David Warde-Farley, Sherjil Ozair, Aaron Courville, and Yoshua Bengio. Generative adversarial nets. In *Advances in neural information processing systems*, pages 2672–2680, 2014. 1
- [12] Ishaan Gulrajani, Faruk Ahmed, Martin Arjovsky, Vincent Dumoulin, and Aaron C Courville. Improved training of wasserstein gans. In *Advances in Neural Information Processing Systems*, pages 5767–5777, 2017. 2
- [13] Kaiming He, Xiangyu Zhang, Shaoqing Ren, and Jian Sun. Deep residual learning for image recognition. In *Proceedings of the IEEE conference on computer vision and pattern recognition*, pages 770–778, 2016. 1, 2
- [14] Martin Heusel, Hubert Ramsauer, Thomas Unterthiner, Bernhard Nessler, and Sepp Hochreiter. Gans trained by a two time-scale update rule converge to a local nash equilibrium. In *Advances in Neural Information Processing Systems*, pages 6626–6637, 2017. 2, 5
- [15] Jonathan Huang, Vivek Rathod, Chen Sun, Menglong Zhu, Anoop Korattikara, Alireza Fathi, Ian Fischer, Zbigniew Wojna, Yang Song, Sergio Guadarrama, et al. Speed/accuracy trade-offs for modern convolutional object detectors. In *IEEE CVPR*, volume 4, 2017. 2
- [16] Xun Huang, Ming-Yu Liu, Serge Belongie, and Jan Kautz. Multimodal unsupervised image-to-image translation. *arXiv preprint arXiv:1804.04732*, 2018. 2
- [17] Phillip Isola, Jun-Yan Zhu, Tinghui Zhou, and Alexei A Efros. Image-to-image translation with conditional adversarial networks. *arXiv preprint*, 2017. 1, 2, 3, 5, 9
- [18] Tero Karras, Timo Aila, Samuli Laine, and Jaakko Lehtinen. Progressive growing of gans for improved quality, stability, and variation. *arXiv preprint arXiv:1710.10196*, 2017. 1, 2, 5
- [19] Diederik P Kingma and Jimmy Ba. Adam: A method for stochastic optimization. *arXiv preprint arXiv:1412.6980*, 2014. 5
- [20] Karol Kurach, Mario Lucic, Xiaohua Zhai, Marcin Michalski, and Sylvain Gelly. The gan landscape: Losses, architectures, regularization, and normalization. *arXiv preprint arXiv:1807.04720*, 2018. 2, 5
- [21] Christian Ledig, Lucas Theis, Ferenc Huszár, Jose Caballero, Andrew Cunningham, Alejandro Acosta, Andrew P Aitken, Alykhan Tejani, Johannes Totz, Zehan Wang, et al. Photo-realistic single image super-resolution using a generative adversarial network. In *CVPR*, volume 2, page 4, 2017. 1, 2
- [22] Minjun Li, Haozhi Huang, Lin Ma, Wei Liu, Tong Zhang, and Yugang Jiang. Unsupervised image-to-image translation with stacked cycle-consistent adversarial networks. In *The European Conference on Computer Vision (ECCV)*, September 2018. 5, 6, 7
- [23] Zeming Li, Chao Peng, Gang Yu, Xiangyu Zhang, Yangdong Deng, and Jian Sun. Detnet: Design backbone for object detection. In *Proceedings of the European Conference on Computer Vision (ECCV)*, pages 334–350, 2018. 2
- [24] Ming-Yu Liu and Oncel Tuzel. Coupled generative adversarial networks. In *Advances in neural information processing systems*, pages 469–477, 2016. 2
- [25] Jonathan Long, Evan Shelhamer, and Trevor Darrell. Fully convolutional networks for semantic segmentation. In *Proceedings of the IEEE conference on computer vision and pattern recognition*, pages 3431–3440, 2015. 5
- [26] Mario Lucic, Karol Kurach, Marcin Michalski, Sylvain Gelly, and Olivier Bousquet. Are gans created equal? a large-scale study. *arXiv preprint arXiv:1711.10337*, 2017. 5
- [27] Luke Metz, Ben Poole, David Pfau, and Jascha Sohl-Dickstein. Unrolled generative adversarial networks. *arXiv preprint arXiv:1611.02163*, 2016. 1, 2
- [28] Takeru Miyato, Toshiki Kataoka, Masanori Koyama, and Yuichi Yoshida. Spectral normalization for generative adversarial networks. *arXiv preprint arXiv:1802.05957*, 2018. 2, 5
- [29] Takeru Miyato and Masanori Koyama. cgans with projection discriminator. *arXiv preprint arXiv:1802.05637*, 2018. 2
- [30] Sebastian Nowozin, Botond Cseke, and Ryota Tomioka. f-gan: Training generative neural samplers using variational divergence minimization. In *Advances in Neural Information Processing Systems*, pages 271–279, 2016. 1, 2
- [31] Augustus Odena, Christopher Olah, and Jonathon Shlens. Conditional image synthesis with auxiliary classifier gans. *arXiv preprint arXiv:1610.09585*, 2016. 2

- [32] George Papandreou, Iasonas Kokkinos, and Pierre-André Savalle. Modeling local and global deformations in deep learning: Epitomic convolution, multiple instance learning, and sliding window detection. In *Proceedings of the IEEE Conference on Computer Vision and Pattern Recognition*, pages 390–399, 2015. [2](#)
- [33] Alec Radford, Luke Metz, and Soumith Chintala. Unsupervised representation learning with deep convolutional generative adversarial networks. *arXiv preprint arXiv:1511.06434*, 2015. [2](#)
- [34] Scott Reed, Zeynep Akata, Xinchun Yan, Lajanugen Logeswaran, Bernt Schiele, and Honglak Lee. Generative adversarial text to image synthesis. *arXiv preprint arXiv:1605.05396*, 2016. [2](#)
- [35] Scott E Reed, Zeynep Akata, Santosh Mohan, Samuel Tenka, Bernt Schiele, and Honglak Lee. Learning what and where to draw. In *Advances in Neural Information Processing Systems*, pages 217–225, 2016. [2](#)
- [36] Tim Salimans, Ian Goodfellow, Wojciech Zaremba, Vicki Cheung, Alec Radford, and Xi Chen. Improved techniques for training gans. In *Advances in Neural Information Processing Systems*, pages 2234–2242, 2016. [2](#)
- [37] Tim Salimans, Han Zhang, Alec Radford, and Dimitris Metaxas. Improving gans using optimal transport. *arXiv preprint arXiv:1803.05573*, 2018. [1](#), [2](#)
- [38] Swami Sankaranarayanan, Yogesh Balaji, Arpit Jain, Ser Nam Lim, and Rama Chellappa. Learning from synthetic data: Addressing domain shift for semantic segmentation. In *The IEEE Conference on Computer Vision and Pattern Recognition (CVPR)*, 2018. [1](#)
- [39] Wenzhe Shi, Jose Caballero, Ferenc Huszár, Johannes Totz, Andrew P Aitken, Rob Bishop, Daniel Rueckert, and Zehan Wang. Real-time single image and video super-resolution using an efficient sub-pixel convolutional neural network. In *Proceedings of the IEEE Conference on Computer Vision and Pattern Recognition*, pages 1874–1883, 2016. [1](#)
- [40] Casper Kaae Sønderby, Jose Caballero, Lucas Theis, Wenzhe Shi, and Ferenc Huszár. Amortised map inference for image super-resolution. *arXiv preprint arXiv:1610.04490*, 2016. [2](#)
- [41] Yaniv Taigman, Adam Polyak, and Lior Wolf. Unsupervised cross-domain image generation. *arXiv preprint arXiv:1611.02200*, 2016. [2](#)
- [42] Zhou Wang, Alan C Bovik, Hamid R Sheikh, and Eero P Simoncelli. Image quality assessment: from error visibility to structural similarity. *IEEE transactions on image processing*, 13(4):600–612, 2004. [5](#)
- [43] Yunchao Wei, Huaxin Xiao, Honghui Shi, Zequn Jie, Jiashi Feng, and Thomas S Huang. Revisiting dilated convolution: A simple approach for weakly-and semi-supervised semantic segmentation. In *Proceedings of the IEEE Conference on Computer Vision and Pattern Recognition*, pages 7268–7277, 2018. [2](#), [4](#)
- [44] Sanghyun Woo, Jongchan Park, Joon-Young Lee, and In So Kweon. Cbam: Convolutional block attention module. In *Proc. of European Conf. on Computer Vision (ECCV)*, 2018. [2](#)
- [45] Maoke Yang, Kun Yu, Chi Zhang, Zhiwei Li, and Kuiyuan Yang. Densespp for semantic segmentation in street scenes. In *Proceedings of the IEEE Conference on Computer Vision and Pattern Recognition*, pages 3684–3692, 2018. [2](#)
- [46] Zichao Yang, Xiaodong He, Jianfeng Gao, Li Deng, and Alex Smola. Stacked attention networks for image question answering. In *Proceedings of the IEEE Conference on Computer Vision and Pattern Recognition*, pages 21–29, 2016. [2](#)
- [47] Zili Yi, Hao (Richard) Zhang, Ping Tan, and Minglun Gong. Dualgan: Unsupervised dual learning for image-to-image translation. In *ICCV*, pages 2868–2876, 2017. [3](#)
- [48] Han Zhang, Ian Goodfellow, Dimitris Metaxas, and Augustus Odena. Self-attention generative adversarial networks. *arXiv preprint arXiv:1805.08318*, 2018. [2](#)
- [49] Han Zhang, Tao Xu, Hongsheng Li, Shaoting Zhang, Xiaolei Huang, Xiaogang Wang, and Dimitris Metaxas. Stackgan: Text to photo-realistic image synthesis with stacked generative adversarial networks. *arXiv preprint*, 2017. [2](#)
- [50] Junbo Zhao, Michael Mathieu, and Yann LeCun. Energy-based generative adversarial network. *arXiv preprint arXiv:1609.03126*, 2016. [1](#), [2](#)
- [51] Feng Zhu, Hongsheng Li, Wanli Ouyang, Nenghai Yu, and Xiaogang Wang. Learning spatial regularization with image-level supervisions for multi-label image classification. *arXiv preprint arXiv:1702.05891*, 2017. [2](#)
- [52] Jun-Yan Zhu, Taesung Park, Phillip Isola, and Alexei A Efros. Unpaired image-to-image translation using cycle-consistent adversarial networks. *arXiv preprint*, 2017. [1](#), [2](#), [3](#), [5](#)